

**VIABILITY OF A NOVEL STRETCHABLE MICROELECTRODE ARRAY  
FOR EPIMYSIAL IMPLANTATION**

A Thesis  
Presented to  
The Academic Faculty

by

Ashton Leigh Cheek

In Partial Fulfillment  
of the Requirements for a  
BS in Biomedical Engineering in the  
Wallace H. Coulter Department of Biomedical Engineering

Georgia Institute of Technology  
May 2014

COPYRIGHT 2014 BY ASHTON CHEEK

**VIABILITY OF A NOVEL STRETCHABLE MICROELECTRODE ARRAY FOR  
EPIMYSIAL IMPLANTATION**

Approved by:

Dr. Stephen P. DeWeerth, Advisor  
School of Engineering  
*Georgia Institute of Technology*

Dr. T. Richard Nichols  
School of Physiology  
*Georgia Institute of Technology*

Date Approved: April 24, 2014

## **ACKNOWLEDGEMENTS**

This work was supported in part by NIH Grants EB006179 and SBIR NS071894-01. The authors would like to thank C.S. Shafor and S. Rajaraman for assisting with sMEA fabrication, and the Ferro Corporation for their generous donation of silver flakes.

# TABLE OF CONTENTS

	Page
ACKNOWLEDGEMENTS	iii
LIST OF TABLES	v
LIST OF FIGURES	vi
SUMMARY	vii
 <u>CHAPTER</u>	
1 INTRODUCTION	1
2 EXPERIMENTAL	2
Adhesion Test sMEA Fabrication	2
Adhesion Pull-Off Test	4
Adhesion Simulated Contraction Test	5
Adhesion Data Analysis	5
Muscle Stimulation and Recording	6
Muscle Contraction Video Analysis	7
Trace Fabrication	8
Tensile Strain v. Resistance Test	8
Tensile Strain v. Resistance Analysis	9
3 RESULTS AND DISCUSSION	11
sMEA Adhesion	11
sMEA Implantation Effect on Muscle Contraction	13
sMEA Trace Tensile Strain v. Resistance Relationship	14
4 CONCLUSION	17
REFERENCES	18

## LIST OF TABLES

	Page
Table 1: Electrode design dimensions	3
Table 2: Peak forces experienced by fabricated MEAs	12

## LIST OF FIGURES

	Page
Figure 1: Adhesion pull-off test setup and Adhesion simulated contraction test	4
Figure 2: Placement of markers on the cat gastrocnemius	7
Figure 3: Tensile strain v. resistance test setup	9
Figure 4: Average change in muscle length during contraction	13
Figure 5: Average change in muscle width during contraction	14
Figure 6: Tensile strain v. resistance of 500 micrometer traces stretched until failure	15
Figure 7: Tensile strain v. resistance of 1000 micrometer traces stretched until failure	15
Figure 8: Tensile strain v. resistance of 500 micrometer traces through three cycles	16
Figure 9: Tensile strain v. resistance of 1000 micrometer traces through three cycles	16

## SUMMARY

Stretchable microelectrode arrays (sMEAs) have been identified for use as neuroprosthetics to treat paralysis. Previous research has focused on assessment of electrical viability and biocompatibility of a novel sMEA device design. However, the mechanical functionality of the device, when implanted epimysially, has yet to be characterized. The device consists of stainless steel arrowhead-shaped electrodes with barbs to promote adhesion to the surface of muscle. A polydimethylsiloxane (PDMS) substrate is used to promote conformation to the muscle surface and stretching of the device alongside muscle movement. Silver PDMS traces are used as stretchable circuits for the device. The adhesive ability of the device, the effect of the device on muscle contraction, and the tensile strain v. resistance relationship of the stretchable traces are assessed. The ninth electrode design is found to be the best design for adhesion of the device epimysially amongst eleven other electrode designs. Epimysial implantation of the device on cat gastrocnemius is not found to significantly affect muscle contraction. The silver PDMS traces are found to fail at 90% strains on average and resistance increases with strain. Stretching cycles of 50% strain are found to consistently increase the base resistance of traces.

# **CHAPTER 1**

## **INTRODUCTION**

Stretchable microelectrode arrays (sMEAs) have been identified for use as neuroprosthetics to treat paralysis [1]. Previous research has focused on assessment of electrical viability and biocompatibility of a novel sMEA device design [2-4]. However, the mechanical functionality of the device, when implanted epimysially, has yet to be characterized. The device consists of stainless steel arrowhead-shaped electrodes with barbs to promote adhesion to the surface of muscle [5], a polydimethylsiloxane (PDMS) substrate to promote conformation to the muscle surface and stretching of the device alongside muscle movement, and silver PDMS traces [4]. The silver PDMS consists of silver particles suspended in PDMS that conduct electricity based on their proximity to other particles [4]. This mixture allows for a stretchable circuit. However, stretching of the traces leads to an increased distance between silver particles, which could potentially increase the resistance of the traces. Epimysial implantation of the device could potentially lead to detachment from the tissue, altered contraction of surrounding muscle, or potential electrical failure of the device as a result of stretching. To address these potential issues, the adhesive ability of the device, the effect of the device on muscle contraction, and the tensile strain v. resistance relationship of the stretchable traces will be assessed.



## **CHAPTER 2**

### **EXPERIMENTAL**

#### **Adhesion Test sMEA Fabrication**

Eleven different electrodes varying with base thickness and barb width (Table 1) were created in SolidWorks and cut from sheets of stainless steel. The electrodes were then pickled in hydrofluoric acid and bent to 90 degree angles. A gold-plated silicone mold was then sprayed with non-silicone mold release and allowed to sit. Silver PDMS was then mixed using silver flakes, PDMS 184 base, and PDMS 184 curing agent. The PDMS was mixed prior to the addition of silver flakes at a 10:1 weight ratio of base to curing agent. Silver flakes were added and mixed at a 4:1 weight ratio to the PDMS mixture. After being mixed thoroughly for a duration of five minutes to make sure that the silver particles were evenly distributed in the mixture, the surface of the mold was thoroughly wiped to remove the mold release from all but the inside of mold. Silver PDMS was then applied to the mold and placed in a vacuum for 40 minutes to remove air bubbles from the mixture.

Electrode Design	Shaft Width (mm)	Barb to Barb Distance (mm)	Base to Tip Distance (mm)
1	0.484	1.1747	2.119
2	0.484	0.9845	2.019
3	0.484	0.7942	2.019
4	0.434	1.1747	2.119
5	0.434	0.9845	2.019
6	0.434	0.7942	2.019
7	0.384	1.1747	2.119
8	0.384	0.9845	2.019
9	0.384	0.7942	2.019
10	0.234	1.1747	2.119
11	0.234	0.9845	2.019

*Table 1: Electrode design dimensions*

After removal from the vacuum, a squeegee was used to remove excess silver PDMS from the mold. Electrodes were then dipped in silver PDMS and uniformly attached to the mold under a microscope. The mold was placed into an oven to cure at 150 degrees Celsius for 16 minutes. Afterwards the mold was sent to have PDMS evenly spun across the surface at a uniform thickness.

The PDMS substrate was then lifted from the mold along with the traces and electrodes. Silver PDMS was applied in small mounds to the back of the electrodes and cured in an oven. PDMS 186 was mixed at a 10:1 ratio of base to curing agent and spun for one minute at 1.0 rcf in a centrifuge to remove bubbles. It was then applied in small mounds on top of the previously applied silver PDMS mounds. While the device was cured in an oven for 25 minutes at 100 degrees Celsius, PDMS 184 was mixed at a 10:1 ratio. After removing the device from the oven, the PDMS 184 mixture was thinly applied to the back of the device with a nitrile glove. The device was then cured in an oven for 45 minutes at 100 degrees Celsius and excess PDMS was later cut off of the

device. Eleven different sMEAs were fabricated using this method such that each sMEA used a different variation of the eleven electrode designs.

### **Adhesion Pull-Off Test**

A single chicken muscle unit was prepared from store-bought chicken legs. The muscle was fixed onto a sterile plate using surgical thread and fixed into place onto the bottom arm of a uniaxial tension machine (Fig. 1). The eleven sMEAs were tested in random order by attaching the trace end of the device to the top arm of the tension machine. The device was then pulled upward at a steady rate of 0.3 mm/s for 1.5 minutes or until the device completely separated from the tissue. The forces required to pull the device off were measured by a force transducer and recorded. Three trials were performed for each sMEA ( $n = 3$ ).

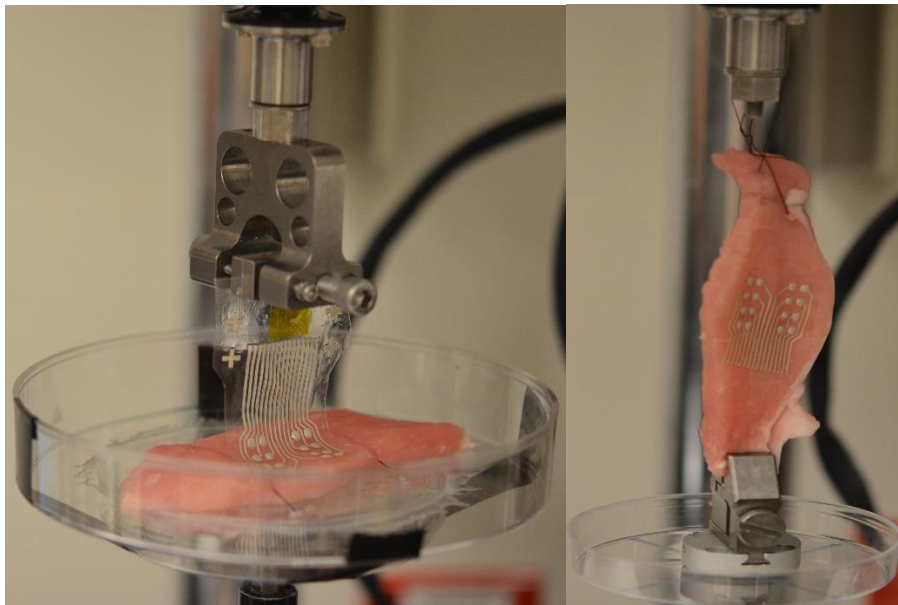


*Figure 1: Adhesion pull-off test setup (Image to the left), Adhesion simulated contraction test (Image to the right)*

### **Adhesion Simulated Contraction Test**

A single chicken unit and pork muscle unit were prepared from store-bought chicken legs and boneless pork chops. The chicken tissue had an outer layer of fascia sheathing the muscle, while the pork tissue did not. When tested, the tissues were attached at each end to the upper and lower arms of the tension machine (Fig. 1). The machine was set to pull the muscles to tension and then to a relaxed state starting at the lowest and highest naturally occurring frequencies of gastrocnemius in humans during normal exercising activities. These frequencies were calculated for an adult male at a height of 5'9'' and of average weight. Each sMEA was implanted onto the muscle tissue and allowed to run through the simulated muscle contractions for ten minutes. The time at which the device separated from the tissue was recorded along with the conditions that triggered separation. If the device did not separate, the frequency was doubled up to eight times the highest naturally occurring frequency or until separation occurred during the contractions. If the device still did not separate, different configurations and external forces were applied to assess conditions necessary for separation of the device from the tissue.

### **Adhesion Data Analysis**

The maximum force experienced for each trial of the eleven sMEA designs was determined by analyzing the data with Microsoft Excel. The peak forces for each of the three trials were then averaged together for each device and the means and standard errors calculated. The best electrode design was then selected based on a qualitative assessment based on maximal average peak adhesive force and minimal standard error.

Observations made during the experiment concerning the number of electrodes that would adhere to tissue for each trial also factored into the qualitative assessment of the electrode designs.

### **Muscle Stimulation and Recording**

All experimental procedures within this study were conducted in accordance with the guidelines of the National Institutes of Health and the Georgia Tech Institutional Animal Care and Use Committee. The best performing sMEA from the adhesion pull-off test was used for this experiment. Markers cut from brightly colored paper and laminated with tape were sutured to cat gastrocnemius along the horizontal and vertical lines of symmetry (Fig. 2). The gastrocnemius of a decerebrated cat was stimulated at 8V for five seconds without the sMEA and recorded using a camera. This was done six times and the muscle was allowed to sit for one and a half minutes between stimulations. The device was then implanted perpendicularly to the muscle's line of action. The muscle was again stimulated at 8V for five seconds and recorded six times with one and a half minute resting periods between stimulation. The device was then re-implanted into the muscle diagonally at 60 degrees from its original position. The muscle was again stimulated at 8V for five seconds and recorded six times with one and a half minute resting periods between stimulation.

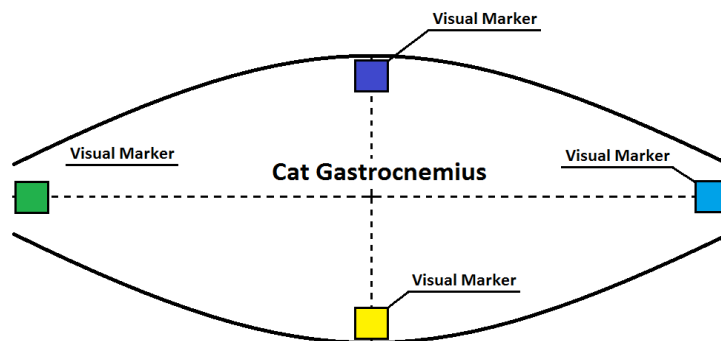


*Figure 2: Placement of markers on the cat gastrocnemius.*

### **Muscle Contraction Video Analysis**

A computer vision algorithm was developed in LabVIEW using Vision Assistant to track different colored rectangular markers placed along the vertical and horizontal lines of symmetry of cat gastrocnemius in an attempt to measure the changes in length and width experienced by the muscle during contraction. It was then determined that the program introduced too much unnecessary error into the analysis of the videos. A simpler and more accurate method was then used. Video capture images were taken prior to stimulation of the muscle and after stimulation for each of the six samples ( $n = 6$ ) of the three test groups. Images were labeled based on their test group and whether they were initial, before stimulation, or final, after stimulation. The images were then opened in GIMP v2.8 and conversion factors were computed for converting distance in pixels to distance in millimeters using a known distance in the images. The distances between markers were then determined using GIMP's caliper tool to measure the distance from the center of the left-most marker to the center of the right-most marker. The distance from the center of the top-most marker to the center of the bottom-most marker was also measured this way. The values were placed into an excel chart that converted the pixel values to millimeters and took the difference between the final and initial distances for

horizontal, the left and right markers, and vertical distance, the top and bottom markers, to determine the changes in length and width that the muscle underwent during contraction. A one-way ANOVA ( $\alpha = 0.05$ ) was then performed on the data for the change in length and for change in width to determine if a significant difference existed between the muscle contractions of the three groups.

### **Trace Fabrication**

A gold-plated silicone mold was fabricated such that seven 500 micrometer thick and seven 1000 micrometer thick traces could be fabricated. The mold was sprayed with mold release and allowed to sit. Silver PDMS was mixed using silver flakes, PDMS 184 base, and PDMS 184 curing agent. The PDMS was mixed prior to the addition of silver flakes at a 10:1 weight ratio of base to curing agent. Silver flakes were then added and mixed at a 4:1 weight ratio to the PDMS mixture. After being mixed thoroughly for a duration of five minutes to make sure that silver particles were evenly distributed in the mixture, the surface of the mold was wiped to remove mold release from all but the inside of mold. Silver PDMS was then applied to the mold and placed in a vacuum for 40 minutes to remove air bubbles from the mixture. Afterwards a squeegee was used to remove excess silver PDMS from the mold. The mold was then sent to have PDMS evenly spun across the surface at a uniform thickness. Rectangular traces were then cut from the PDMS.

### **Tensile Strain v. Resistance Test**

The traces were wrapped in aluminum foil with a resistance of three Ohms and fixed at each end to clamps that are capable of having the distance between them finely adjusted using screws (Fig. 3). The resistance of the trace was constantly measured by a multimeter, and the trace was stretched by increments of approximately 0.5 mm until the trace experienced mechanical failure. After each step of 0.5 mm, 30 seconds was allowed to pass before recording the resistance. Four samples were tested this way for both trace thicknesses ( $n = 4$ ). Three traces from each group were then set to a length of 20 mm and stretched to 50% strain. The length of the traces was reduced by steps of approximately 0.5 mm until the original 20 mm length was reached. This process was repeated three times and 30 seconds were allowed to pass after each length adjustment before resistance was recorded.

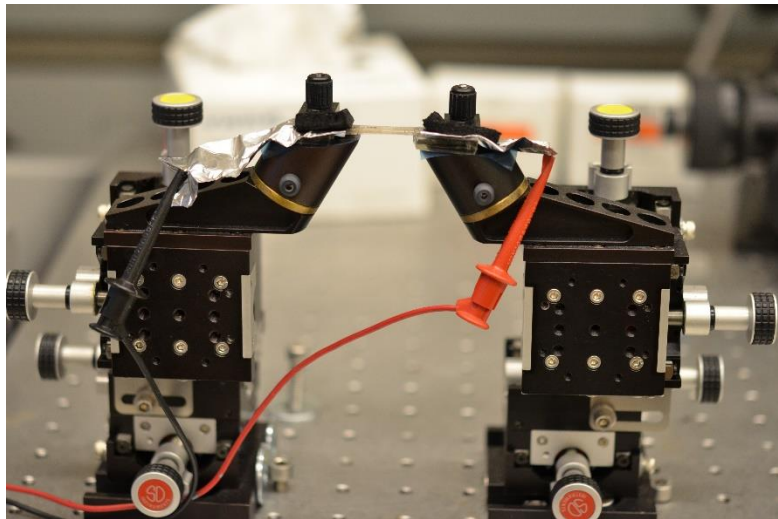


*Figure 3: Tensile strain v. resistance test setup*



### **Tensile Strain v. Resistance Analysis**

For the traces that were stretched until mechanical failure, the length at which failure occurred was recorded in Excel along with the initial length. Strain was computed from these values and averaged together with the failure strain values of the other samples within the respective group. The average strains at which mechanical failure occurred in both groups were then qualitatively compared. The values for resistance and length were plotted against one another to determine the relationship between the two.

For the traces that were set at 20 mm and then stretched to 50% for three cycles, the recorded resistances and lengths were used to create graphs. These graphs were then used for a qualitative assessment of the effect that cycles of 50% strain had on the resistances of the traces. These graphs were also used to determine a relationship between the strain and resistance for 50% strain cycles conducted on the silver PDMS traces.

## **CHAPTER 3**

### **RESULTS AND DISCUSSION**

#### **sMEA Adhesion**

For the pull-off test, the MEAs fabricated with electrode designs one through four experienced complete separation with only a few electrodes managing to adhere to the tissue. The MEAs fabricated with electrode designs five through seven completely separated most of the time with a fourth to a half of the electrodes managing to adhere to the muscle tissue. MEAs fabricated with designs eight, ten, and eleven experienced complete detachment from the tissue some of the time with three quarters of electrodes managing to adhere to the tissue. The MEA fabricated with electrode design nine never experienced complete separation from the tissue and all electrodes managed to adhere to the tissue.

The MEA fabricated with design eleven experienced the highest average peak force and the MEA fabricated with electrode design nine experienced the second highest average peak force (Table 2). However, the MEA fabricated with design nine also experienced the lowest amount of variation between measured peak forces among all groups. It is important that the electrode design used for the device both adhere strongly to muscle tissue and adhere with a consistent amount of adhesive force. Given these constraints, the results of the pull-off test suggest that electrode design number nine is the best electrode design for promoting adhesion of the device to muscle tissue.

Electrode Design	Trial 1 Peak Force (N)	Trial 2 Peak Force (N)	Trial 3 Peak Force (N)	Average Peak Force (N)	Standard Error
1	4.407	3.845	5.580	4.611	0.4426
2	4.616	4.772	4.804	4.731	0.0503
3	4.641	4.658	4.204	4.501	0.1287
4	4.746	4.632	4.722	4.700	0.0301
5	5.031	4.480	5.639	5.050	0.2899
6	5.438	4.807	4.919	5.055	0.1683
7	5.368	5.203	5.682	5.418	0.1217
8	6.415	6.503	5.322	6.080	0.3290
9	6.130	6.037	6.118	6.095	0.0253
10	5.521	4.550	6.46	5.510	0.4775
11	6.405	5.571	6.323	6.100	0.2298

*Table 2: Peak forces experienced by fabricated MEAs when pulled off of chicken muscle tissue.*

The simulated contraction test yielded no major results because none of the MEAs ever detached from the muscle tissue. The simulated contraction test was performed on chicken muscle and pork muscle with the same results and observations. It was observed during both tests that the device would not detach from the tissue at the lowest attempted frequency of contraction or the highest frequency of contraction that the tension machine could support. Multiple configurations for implantation of the device onto the surface were attempted and all yielded the same results. One end of the MEAs was fixed in one place to determine if this condition would cause separation, but it did not. However, upon fixing the position of one end while simultaneously pulling the device perpendicularly to the muscle movement, the device detached after a number of contractions. From this observation, it is hypothesized that previous instances of detachment of the device experienced during contractions of muscle were a result of external forces pulling on the device, such as the wires that were potentially being used to assess the electrical capabilities of the device.

### sMEA Implantation Effect on Muscle Contraction

A one- way ANOVA was performed on the measured changes in the length (Fig. 4) and width (Fig. 5) of cat gastrocnemius with and without a sMEA implanted on the muscle surface ( $\alpha = 0.05$ ). Six samples for each of the three test groups were recorded ( $n = 6$ ). No significant difference between groups was found for the changes in length during muscle contraction for the gastrocnemius ( $p\text{-value} = 0.2037$ ) or for the changes in width ( $p\text{-value} = 0.0619$ ). However, the change in width was close to being significant, especially between the control group and the sMEA position one group. Position one of implanting the sMEA was with the electrode columns arranged along the width of the muscle. This suggests that the sMEA has a slight effect on muscle contraction in the direction with the largest amount of distance between consecutive electrodes. This effect can be mitigated by reducing the thickness of the PDMS substrate.

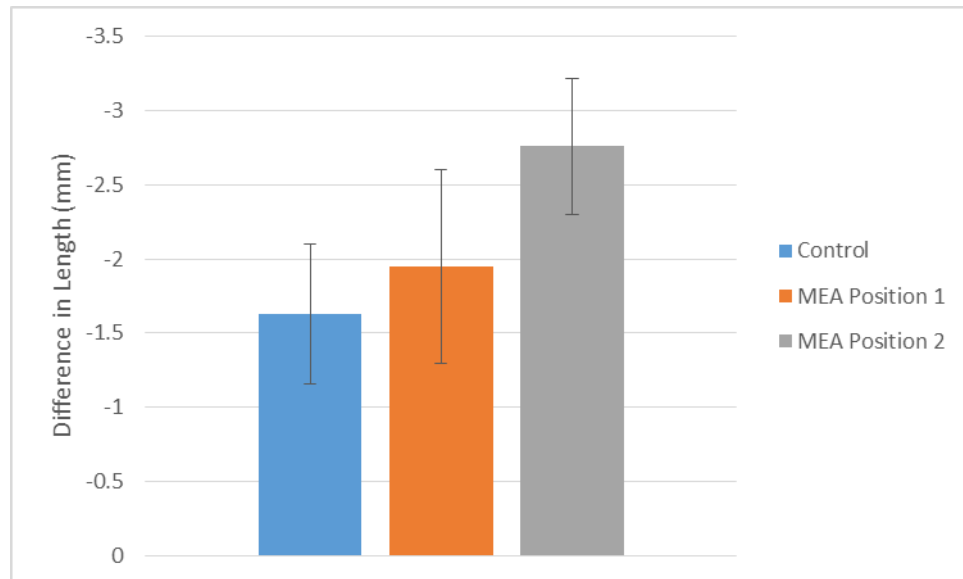


Figure 4: Average change in muscle length during contraction. The bars in the graph represent standard error.

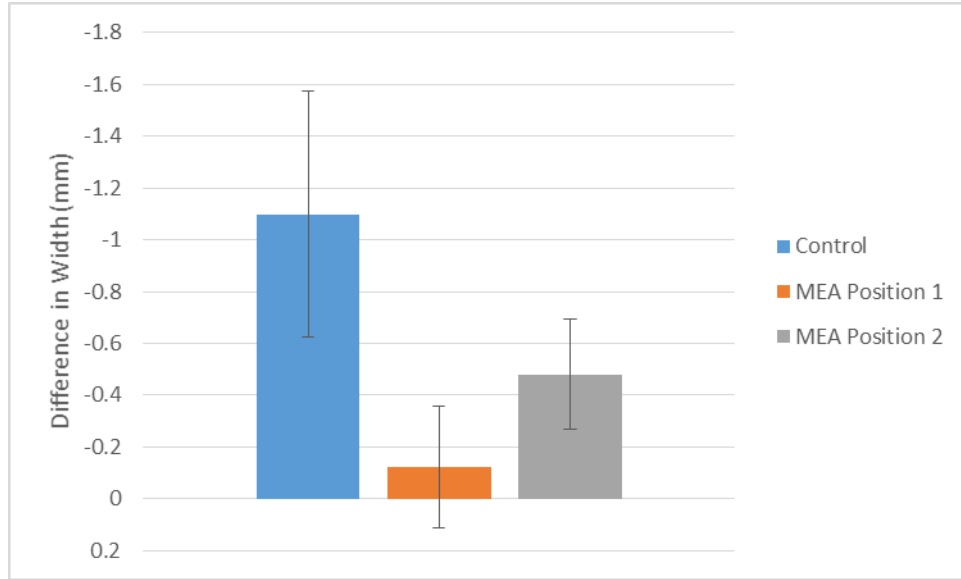


Figure 5: Average change in muscle width during contraction. The bars in the graph represent standard error

### sMEA Trace Tensile Strain v. Resistance Relationship

The average strain of 500 and 1000 micrometer traces when failure occurred was found to be 90% on average. The resistance of the traces tended to increase as the tensile strain increased, as can be seen in Figure 6 and Figure 7. There was at least one sample in both the 500 and 1000 micrometer trace groups that would experience oscillating resistance as the strains increased without necessarily increasing over time. This is likely caused by the random arrangement of the silver particles suspended in the PDMS of the trace. The particles may grow further apart from their neighbors that best promote conductivity, but become closer to particles that were once too far away to enable the transmission of a charge. As the resistances experienced by these samples typically stayed lower than other samples, it would be beneficial for the function of the device to find a way to consistently replicate this effect within traces.

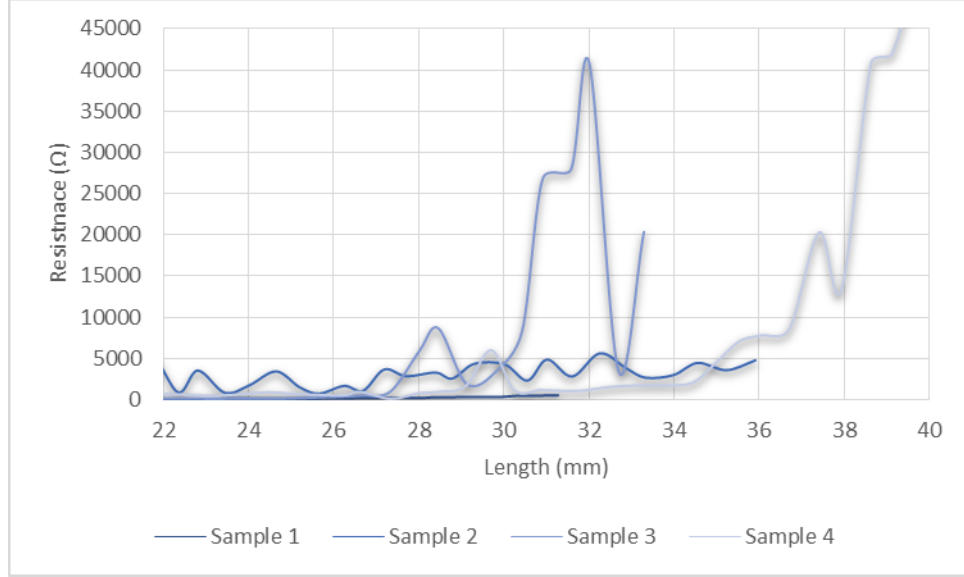


Figure 6: Tensile strain v resistance of 500 micrometer traces stretched until failure.

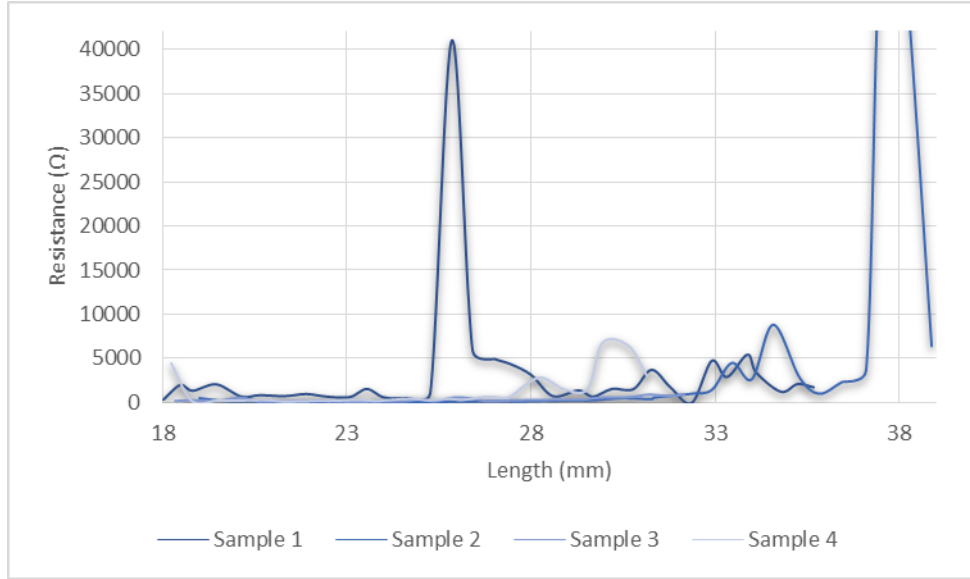


Figure 7: Tensile strain v resistance of 1000 micrometer traces stretched until failure.

For the 500 and 1000 micrometer traces that were stretched to 50% strain and then gradually brought back to 0% strain for three cycles (Fig.8 and Fig. 9), the resistance would typically increase with the number of completed cycles. Also, the resistance began increasing as the traces approached the 25% strain mark and began decreasing at the 10% strain mark. This phenomenon is likely the result of the tensile set properties of the silver PDMS. It is speculated that the consistently increasing resistance is a result of silver

particles never completely returning to their original positions, reducing the number of silver particles in proximity to one another.

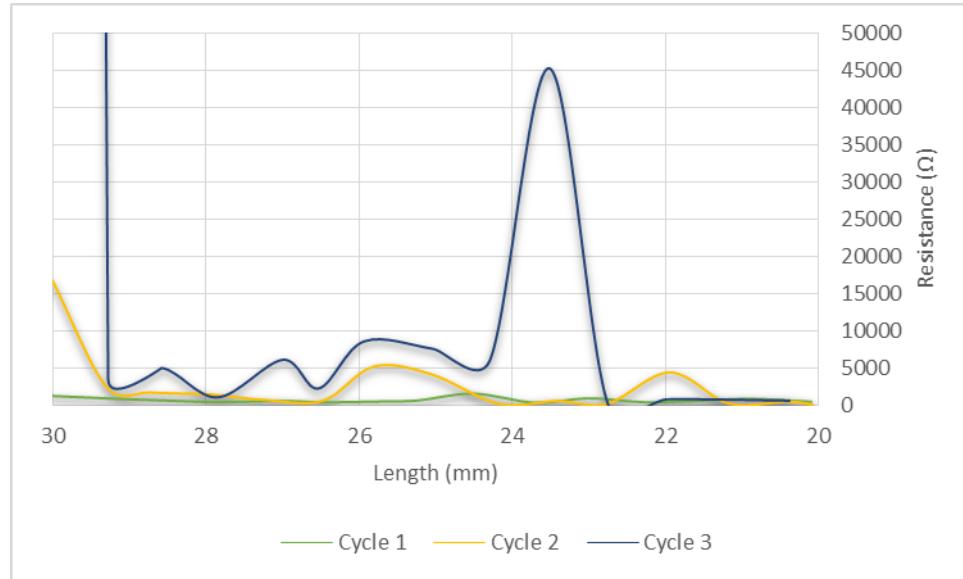


Figure 8: Tensile strain v resistance of 500 micrometer traces through three cycles of stretching up to %50 percent strain.

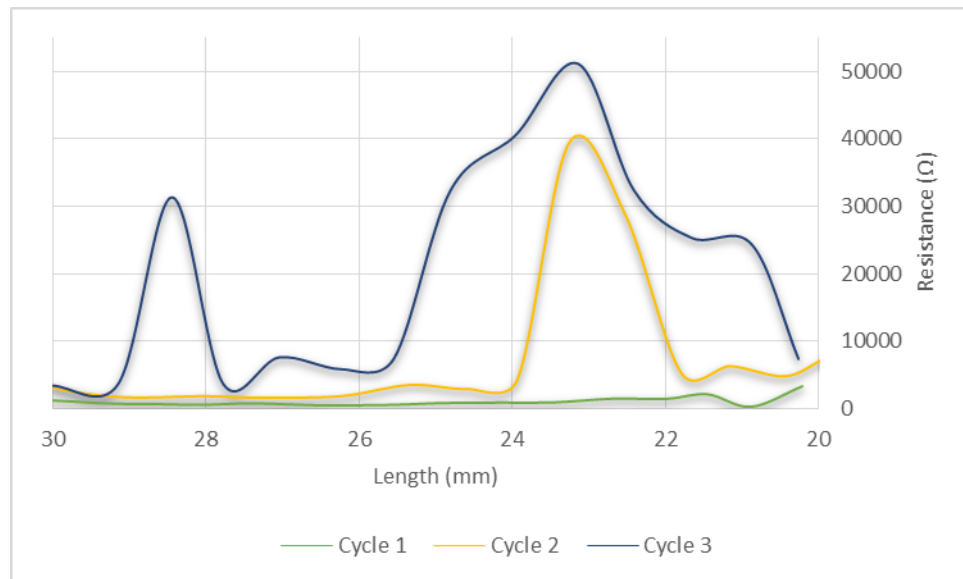


Figure 9: Tensile strain v resistance of 1000 micrometer traces through three cycles of stretching up to 50 percent strain.

## **CHAPTER 4**

### **CONCLUSION**

A novel design for a sMEA was proposed and its mechanical functionality analyzed. Electrode design number nine was found to be the best at promoting adhesion of the device among the eleven electrode designs, and it is proposed that future iterations of the device incorporate this electrode into their design. In addition, it was found that the device does not significantly affect the contraction of cat gastrocnemius when implanted epimysially. However, it is recommended that the PDMS thickness be reduced to mitigate the slight effect that the device has on muscle in the direction covered by the largest distance of consecutive electrodes.

The silver PDMS traces for both 500 and 1000 micrometer thicknesses were found to fail mechanically at 90% on average and the resistance of traces was observed to increase with strain. Additionally, stretching cycles of 50% strain were found to consistently increase the overall resistance of traces with each cycle. The proposed changes to the device design will optimize the device for epimysial implantation by augmenting its ability to adhere to muscle and reducing its potential effect on muscle contractions.



## REFERENCES

- [1] Cheung, K. C. (2007). Implantable microscale neural interfaces. *Biomedical Microdevices*, 9(6), 923–938. doi:10.1007/s10544-006-9045-z
- [2] Guo, L., Givanasen, G. S., Liu, X., Tuthill, C., Nichols, T. R., & DeWeerth, S. P. (2013). A PDMS-Based Integrated Stretchable Multielectrode Array (isMEA) for Neural and Muscular Surface Interfacing. Retrieved from [http://ieeexplore.ieee.org/xpls/abs\\_all.jsp?arnumber=6197244](http://ieeexplore.ieee.org/xpls/abs_all.jsp?arnumber=6197244)
- [3] Guo, L., Givanasen, G., Tuthill, C., Nichols, T. R., & DeWeerth, S. P. (2011). A low-cost, easy-fabricating stretchable microneedle-electrode array for intramuscular recording and stimulation. In *Neural Engineering (NER), 2011 5th International IEEE/EMBS Conference on* (pp. 562–565). Retrieved from [http://ieeexplore.ieee.org/xpls/abs\\_all.jsp?arnumber=5910610](http://ieeexplore.ieee.org/xpls/abs_all.jsp?arnumber=5910610)
- [4] Givanasen, G. S., Aguilar, R. J., Guo, L., Karnati, C., Rajaraman, S., Nichols, T. R., & DeWeerth, S. P. (n.d.). Development of a stretchable, penetrating electrode array for measuring intramuscular electromyographic activity. (Unpublished Research)
- [5] Cho, W. K., Ankrum, J. A., Guo, D., Chester, S. A., Yang, S. Y., Kashyap, A., ... Karp, J. M. (2012). Microstructured barbs on the North American porcupine quill enable easy tissue penetration and difficult removal. *Proceedings of the National Academy of Sciences*, 109(52), 21289–21294. doi:10.1073/pnas.1216441109